

1 Soft robotics and the quest for modeling the
2 physics of embodied intelligence

3 Gianmarco Mengaldo^{1*}, Federico Renda², Steven Brunton³, Moritz
4 Bächer⁴, Marcello Calisti⁵, Christian Duriez⁶, Gregory S. Chirikjian¹
5 and Cecilia Laschi^{1*}

6 ¹National University of Singapore, Singapore, SG.

7 ²Khalifa University, Abu Dhabi, UAE.

8 ³University of Washington, Seattle, USA.

9 ⁴Disney Research, Zurich, Switzerland.

10 ⁵University of Lincoln, Lincoln, UK.

11 ⁶INRIA, Lille, France.

12 *Corresponding author(s): mpegim@nus.edu.sg; mpeclc@nus.edu.sg;

13 Contributing authors: federico.renda@ku.ac.ae; sbrunton@uw.edu;

14 moritz.baecher@disneyresearch.com; mcalisti@lincoln.ac.uk;

15 christian.duriez@inria.fr; mpegre@nus.edu.sg;

16 **Abstract**

17 Embodied intelligence, or intelligence that requires and leverages a
18 physical body, is ubiquitous in biological systems, both in animals
19 and plants. Through embodied intelligence, biological systems effi-
20 ciently interact with and use their surrounding environment to let
21 adaptive behaviour emerge. In soft robotics, this is a well-known
22 paradigm, whose mathematical description and consequent compu-
23 tational modelling remain elusive. We argue that filling this gap
24 will enable full uptake of embodied intelligence in soft robots.
25 The resulting models can be used for design and control purposes.
26 In this perspective, we provide a concise guide to the main mathe-
27 matical modelling approaches, and consequent computational modeling
28 strategies, that can be used to describe soft robots and their physi-
29 cal interactions with the surrounding environment, including fluid and
30 solid media. The goal of this perspective is to convey the challenges
31 and opportunities within the context of modeling the physical inter-
32 actions underpinning embodied intelligence. We emphasize that inter-
33 disciplinary work is required, especially in the context of fully coupled
34 robot-environment interaction modeling. Promoting this dialogue across
35 disciplines is a necessary step to further advance the field of soft robotics.

36
37

Keywords: Soft robotics, Embodied intelligence, Mathematical modeling,
Computational modeling, Computational physics

38 1 Introduction

39 Soft robotics is largely motivated by the functional role of soft tissues in liv-
40 ing organisms [1]. Life has had millions of years to adapt to their surrounding
41 environment and co-evolve nervous and muscle-skeletal systems to achieve
42 task-efficient performance, synergistically. We observe that living beings are
43 soft and compliant, and we argue that this is instrumental to their embodied
44 intelligence [2]. According to this modern view of intelligence, the physi-
45 cal body play a much larger role in shaping intelligence, since a part of
46 sensory–motor behaviour emerges from its interaction with the surrounding
47 environment, with minimal or no involvement of the nervous system. Soft bio-
48 logical systems use their complex internal body structure to efficiently leverage
49 physical interactions with the external environment and achieve the desired
50 actions. Indeed, external interaction forces, instead of being treated as distur-
51 bances needing compensation, are used for the intended movements [3]. As an
52 example, in locomotion, gravity is exploited for stepping forward, and adapta-
53 tion to uneven terrains is provided by compliant elements within the leg joints,
54 with limited need for active inputs from the central nervous system. Similarly,
55 octopuses, an iconic model for soft robotics, adopt highly effective unfolding
56 arm reaching movements by leveraging the buoyancy and interaction forces
57 from the water surrounding them.

58 Embodied intelligence is a well-known paradigm in robotics and in soft
59 robotics. In a typical robot sensory–motor behaviour scheme, we can consider

60 a sensory system perceiving the environment, controllers processing the incom-
 61 ing information and planning a motor action, and then a mechanical system
 62 that executes motor actions in the physical environment. Embodied intelli-
 63 gence can be seen as the mechanical feedback from the environment, directly
 64 onto the mechanical system of the robot physical body, with no involvement
 65 of controllers or processing (see Fig. 1, from [2]). This view gives a clear per-
 66 ception of how powerful embodied intelligence can be in simplifying robot
 67 sensory–motor behaviour and increasing overall robot efficiency and effective-
 68 ness. All this works if we assume that a soft, compliant body receives, and
 69 does not reject, the mechanical feedback from the environment.

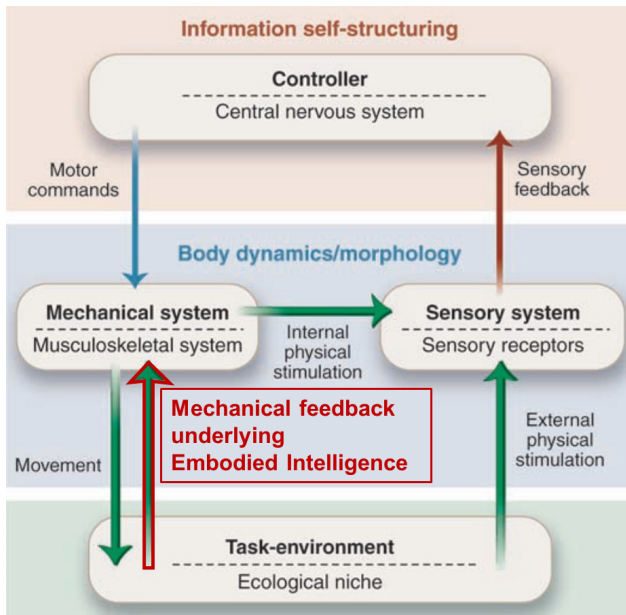


Fig. 1: In a typical robot sensory–motor scheme, embodied intelligence can be seen in the mechanical feedback received by the physical body from the environment. It allows closing a very short control loop, by-passing most of the computational processes. (Reprinted with permission from [2] and adapted).

70 How to systematically design embodied intelligence into soft robots is one
71 of the current challenges in the field. We argue that this goal can be achieved
72 by means of a mathematical description of the physical interactions charac-
73 terizing embodied intelligence. Related computational modeling would enable
74 simulations to be used for both design and control purposes.

75 The task of constructing this modeling framework is not an easy one. Take
76 as an example a soft arm immersed in a fluid and interacting with solids (see,
77 e.g., the octopus in Fig. 2). To describe and model the physics underlying
78 embodied intelligence, it is necessary to consider:

- 79 • the continuous deformations of the arm deriving from muscle activations,
- 80 • the coupled interaction of the arm with the fluid, when e.g., the arm reaches
81 out for target objects and moves the water, and the water contributes to its
82 deformation,
- 83 • the interactions of the soft arm with solids (rigid or deformable), like the
84 seafloor when walking, or external objects when grasping.

85 The description of these three points present a number of crucial challenges.

86 First, the problem is inherently multiphysics, due to the physically hetero-
87 geneous nature of interactions underlying embodied intelligence. In fact, one
88 needs to take into account the physics of the soft body and the dynamics of
89 muscle activation, the flow physics and its coupling with the soft body, and
90 the physics describing contact and adhesion between two solids. This poses
91 the critical challenge (and opportunity) of interdisciplinary work across multi-
92 ple communities, ranging from robotics, fluid dynamics, structural mechanics,
93 tribology, and contact mechanics. These fields typically have their own cus-
94 toms and terminology, and cross-fertilization can prove difficult, yet will be
95 beneficial to bring advances in modeling embodied intelligence.

96 Second, the problem is multiscale, as the number of scales one needs to
97 describe may range from millimeters to meters. For instance, in our example
98 the arm reaching movement may undergo an overall displacement of several
99 centimeters. Yet, the description of the deformation of the soft body, and
100 its interaction with the flow and solid, may require a much finer descrip-
101 tion to accurately capture its behaviour. To this end, fast computational
102 methods to solve multiscale problems are required. Integration with the sci-
103 entific computing and applied mathematics communities may therefore prove
104 important.

105 Multiphysics and multiscale problems are notoriously challenging but have
106 successfully been conquered in some fields, including the aerospace industry,
107 biomedical engineering, and material science, to cite a few. In the context
108 of soft robotics, these problems have yet to be addressed, although promis-
109 ing advances have been made. Some of the factors that make modelling
110 particularly difficult here are: i) how the actuation forces are designed and
111 mathematically modelled to achieve a desired action, and how the surround-
112 ing environment influences them; ii) large deformations of nonlinear materials
113 and their coupled interactions with the surrounding medium, which leads to
114 high-dimensional models that are often prohibitively expensive to simulate
115 and use inside control loops; and iii) partially known interfacial physics and
116 unmodeled dynamics – e.g., nonlinear friction mechanisms for solid–solid inter-
117 action, and turbulent drag for fluid–structure interaction. In addition, the
118 range of morphologies (e.g., arms, fingers, legs, fins), materials (e.g., hypere-
119 lastic, heterogeneous, functional), abilities (e.g., reaching, grasping, walking,
120 morphing, growing, swimming, jumping, crawling, digging) and intended
121 applications (e.g., healthcare, manufacturing, underwater sensing and manipu-
122 lation, scientific exploration, entertainment) is extremely diverse, exacerbating

123 the complexity of the modelling task. The latter aspect may lead to staggered
124 and application-specific modelling strategies, that may not be beneficial to the
125 soft robotics field.

126 In this paper, to support our argument of distilling embodied intelligence
127 into physical interactions, we provide a concise guide to the latter and to their
128 underlying mathematical models. In particular, we present and discuss the
129 most prominent models that describe 1) the interactions of soft robot compo-
130 nents (including actuators) that lead to efficient movements and deformation,
131 and 2) the robot interactions with the surrounding environment. We refer to
132 the former as *internal interactions*, and the latter as *external interactions*,
133 where the environment can be constituted by fluid or a solid.¹ To introduce the
134 models underlying the physical interactions found in embodied intelligence, we
135 use the octopus depicted in Fig. 2 as a proxy for a general biological or soft
136 robotics system.

¹We note that the surrounding environment may be constituted of heterogeneous granular material. In this case, one may need to rely on different methods than the ones presented in this paper. Yet, the case of solid or fluid media is sufficiently general to provide an effective guide on modeling interactions between soft bodies and the environment.

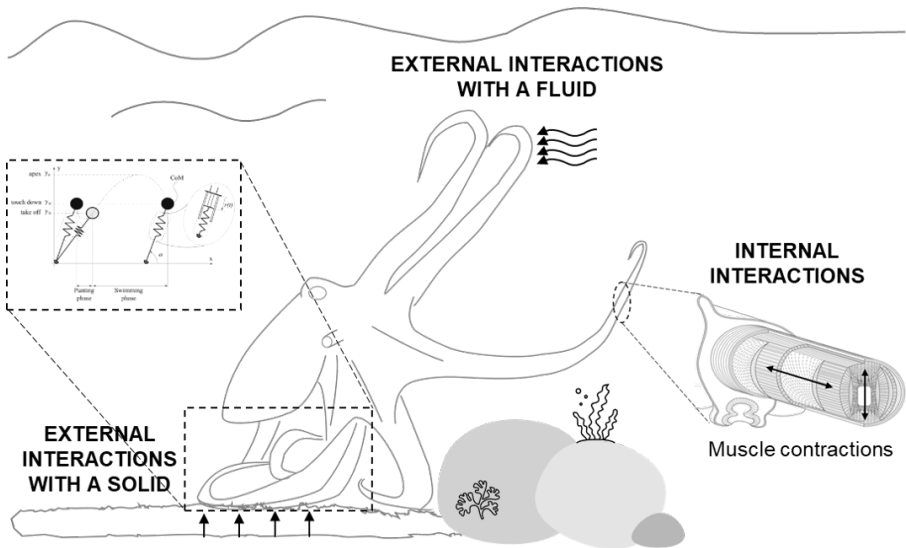


Fig. 2: An illustration of our scope in modeling the physics of embodied intelligence. We use an octopus as a proxy for a general soft body, in its environment, where we highlight the three key modeling areas that contribute to a substantial insight of embodied intelligence: *internal interactions*, and *external interactions* models, either with a fluid medium or a solid support. Internal interactions refer to the deformations of the soft body induced by actuators, or muscles. External interactions refer to the action of the external environment (fluid or solid) on the soft body. We also highlight how the accurate description of internal and external interactions can lead to low-dimensional models that capture the soft body behaviour with a reduced number of state variables.

137 1.1 A Mathematical Framework for Modeling of Soft Robots

The mathematical framework adopted belongs to the realm of mechanics that is at the foundations of physical interactions in both solids and fluids. To describe the mechanics of physical systems there are two views, Lagrangian and Eulerian. In the former, one tracks the trajectories of particles, while in the latter one observes the particle velocities at a fixed point in space. The

Lagrangian setting is commonly used in classical solid mechanics, while the Eulerian setting is commonly used in fluid mechanics. These two views allow us to introduce an abstract mathematical formalism for the soft body subject to *internal* and *external* interactions that consists of a set of differential equations:

$$\mathcal{D}\mathbf{q}_{\text{sb}} = \mathcal{N}_{\text{sb}} + \mathcal{C}_{\text{int}} + \mathcal{C}_{\text{ext}}, \quad \text{in } \Omega_{\text{sb}} \quad (1)$$

138 Equation (1), along with suitable initial and boundary conditions, can
 139 describe both models arising in continuum mechanics and multibody dynam-
 140 ics in the soft body domain Ω_{sb} . The former typically yields a set of partial
 141 differential equations, while the latter a set of ordinary differential equations.
 142 Depending on the approach used, the variables \mathbf{q}_{sb} , that describe the soft body
 143 (sb), can have a different meaning. For instance, in a Lagrangian view, \mathbf{q}_{sb} rep-
 144 represents the position and momentum of material particles, while in an Eulerian
 145 view, \mathbf{q}_{sb} is the observed velocity at each given point. \mathcal{D} is a differential oper-
 146 ator that may be a partial (∂) or a total (d) derivative (including a material
 147 derivative D), of first or second order.

148 \mathcal{N}_{sb} is a nonlinear term that describes the soft body (sb) mechanics, which
 149 may depend on \mathbf{q}_{sb} , its partial derivatives with respect to spatial coordinates
 150 \mathbf{x} , time t , and by a set of tunable constants such as viscosity, stiffness, and
 151 other actuation and material parameters.

152 \mathcal{C}_{int} is a coupling term that accounts for internal (int) interactions (e.g.,
 153 actuation forces for tendons or pressure of pneumatic chambers). \mathcal{C}_{ext} is a
 154 coupling term that accounts for external (ext) interactions (e.g., contact with
 155 external solids or interactions with the surrounding medium).

156 While equation (1) may not be the standard way of introducing models
 157 in the realm of soft robotics, it allows a sufficiently general mathematical

158 framework that can be used as a basis to construct a unified formalism for
159 the multiphysics of internal and external interactions. We divided the right-
160 hand side into a nonlinear term \mathcal{N}_{sb} , and two coupling terms \mathcal{C}_{int} and \mathcal{C}_{ext} ,
161 to emphasize the mechanics of the soft body (through \mathcal{N}_{sb}) and its coupling
162 not only with internal (through \mathcal{C}_{int}) but also with external systems (through
163 \mathcal{C}_{ext}). In particular, \mathcal{C}_{int} , and \mathcal{C}_{ext} can constitute forcing terms, that results
164 from lumping the interactions into simplified terms, or can be terms coupling
165 the equation describing the soft body (1) to additional equations describing
166 the physics of internal and/or external interactions (e.g., actuators, and the
167 surrounding environment). These interactions could be for instance described
168 by equality and inequality constraints, especially when the soft body is in
169 contact with a medium. In this case, the constraints can be embedded into the
170 equations by means of, e.g., Lagrange multipliers, and encapsulate the physics
171 of interactions. For example, frictional contact between two surfaces is best
172 modeled with inequality constraints which become active as soon as a soft
173 body is in contact with either itself or the environment.

174 Starting from equation (1), in the following we introduce the models and
175 solution methods adopted for *internal* and *external* interactions. More specif-
176 ically, the outline of this paper is as follows. In section 2, we detail the models
177 for internal interactions, describing both the models for soft-body mechanics
178 (i.e., \mathcal{N}_{sb}), and the internal interactions with actuators (i.e., \mathcal{C}_{int}). In section 3,
179 we describe the models for external interactions (i.e., \mathcal{C}_{ext}). In section 4, we
180 outline how these models can be used in practice for soft robotics. In section 5,
181 we review the modeling challenges and opportunities described, and draw some
182 conclusions and perspectives.

2 Internal interactions

2.1 Challenges

A soft-bodied system, such as the arm of the octopus depicted in Fig. 2, is composed of a set of sensors and actuators, distributed inside a soft tissue, that work together to achieve a given task. The various sensing and actuation mechanisms interact internally with one another, and they typically operate within a nonlinear and possibly heterogeneous material constituting the soft tissue. We focus here on the fundamental robotics task of modeling the relations between the actuator space and the soft-body deformations. A mathematical model describing internal interactions should therefore capture the robot deformation (i.e., \mathcal{N}_{sb}) produced by the internal actuation forces, where the latter also needs to be accurately represented (i.e., \mathcal{C}_{int}).

The degrees of freedom represented by the internal interactions are only a part of the degrees of freedom of the system. The first step is to describe the physics of actuation in a subspace of the deformable system. Once this space is defined, the key challenges specific to modeling internal interactions are:

1. to model the physics of the actuation in such a way that it can be identified on the real system, and
2. to couple the two physics: the one of the deformation of the structure, and the one of the actuation.

To this end, we take into account the following three main actuation strategies:

Tendons (1D). We consider here a punctual action of a cable or similar tendon-like actuator, which we consider as one-dimensional (1D). If the tension is exerted by a tendon which pulls, it is relatively easy to describe the force field created on a soft robot structure, based on the geometrical path. When

209 a series of tendons are placed on a robot and their input lengths need to be
210 integrated, the problem becomes more complex: since the tendons are coupled,
211 it is necessary to verify that they are tense to exert a force. The tension of
212 one tendon on a structure could slack on other ones. Also the tension inside
213 the tendon is a signed force: we can pull with a tendon, but not push. The
214 algebraic equations, translating the motion of the tendon, lead to constraints
215 of inequality and complementarity. Finally, more advanced models that could
216 be used to replicate the mechanics of the tendons (extension, bending, internal
217 friction, etc.) are neglected to focus on this tensile force.

218 **Flexible fluidic actuators (2D).** In this case, we consider a chamber that
219 deforms when pressurized with a fluid, so that a pressure acts on a surface, and
220 we assume it to be constrained to two-dimensional (2D) deformations. In the
221 same way, for these fluidic actuators, it is possible to directly take into account
222 the pressure exerted in cavities. This pressure is then integrated on the surface
223 of the cavity to calculate a force field applied to the soft robot structure. This
224 approach is often used for pneumatic actuation, based on pressure regulators.
225 On the other hand, in the case of liquid injection, it is often the variation of the
226 cavity volume to constitute the input of the model. As with the tendon case,
227 it is then necessary to add an algebraic equation in the model translating the
228 volume variation. Moreover, the weight exerted by the liquid on the structure
229 can create additional deformations. Finally, one can imagine, in the longer
230 term, coupling the deformation models with dynamic models of the fluid.

231 **Smart materials (3D).** Smart materials are a large class of materials
232 responding to external stimuli, and we consider this as a three-dimensional
233 (3D) actuator. Some smart materials, such as electro-active or electro-ionic
234 polymers, have their internal stress field dependent on an electric field. Other

235 materials, such as shape memory materials, have their constitutive law depen-
 236 dent on temperature. Materials can also be integrated into soft robots that
 237 react to a magnetic field. In all these cases (and possibly in many others, the
 238 field of smart material being vast), the problem is the coupling of the deforma-
 239 tion equations with other equations of physics, like electric or magnetic fields
 240 or temperature diffusion, often at scales that are much smaller than the scale
 241 of the robot.

242 The modeling of those actuators constitutes a challenge *per se*, and their inte-
 243 gration with different soft-body models can be non-trivial. In particular, soft
 244 robots are highly under-actuated (the degrees of freedom associated with actu-
 245 ation are significantly fewer than the degrees of freedom of the soft body).
 246 Therefore, it is frequently required to add algebraic constraints, often associ-
 247 ated with Lagrange multipliers $\mathbf{\Lambda}$ and $\mathbf{\Theta}$, to drive the motion of the soft body
 248 within the actuator space. In this case, the coupling term with the actuators
 249 becomes $\mathcal{C}_{\text{int}} = \mathbf{\Lambda}^T \mathcal{I}_e + \mathbf{\Theta}^T \mathcal{I}_i$, where \mathcal{I}_e and \mathcal{I}_i are equality and inequality
 250 constraints, respectively. The method of the Lagrange multipliers is a strategy
 251 to enforce equality constraints to a functional, in this case equation (1).

252 2.2 Models

253 Two modeling approaches of internal interactions exist in robotics. The first,
 254 called direct modeling approach, starts from the knowledge of the motion
 255 and/or forces in the actuator space and from other unactuated degrees of
 256 freedom to compute the robot shape. The second, known as inverse modeling
 257 approach, starts from a desired shape or position of the robot and calculate
 258 the actuator space in order to reach the desired shape/position.

259 In this section we will focus on the direct modeling approach. The actuator
 260 forces will modify the static equilibrium or the dynamics of the robot.

261 In the following, we introduce the main models that can be used for
 262 describing the soft body mechanics \mathcal{N}_{sb} and how they can be integrated with
 263 the actuation strategies reported above, through \mathcal{C}_{int} . We introduce contin-
 264 uum solid mechanics models (fully 3D or rod/shells) and finite-dimensional
 265 parametrization models and we keep their description at a level general enough
 266 to provide the reader with tools adaptable to most cases. We also introduce
 267 the possible use of data-driven methods for the same modelling problems.

268 *2.2.1 Continuum three-dimensional solid mechanics models*

269 The most general model that captures the full complexity of the soft body is
 270 given by three-dimensional continuum solid mechanics (see Fig. 3(a)). If we
 271 consider equation (1), taking an Eulerian view:

272 \mathcal{D} becomes $\partial/\partial t$, the partial derivative with respect to time t ,

273 \mathbf{q}_{sb} becomes \mathbf{v}_{sb} , representing the velocity field of the soft body,

274 \mathcal{N}_{sb} becomes $\nabla \cdot \boldsymbol{\sigma}_{\text{sb}}$, the divergence of the soft body stress tensor $\boldsymbol{\sigma}_{\text{sb}}$.

275 This equation describes the balance of linear momentum, that is usually com-
 276 plemented by the balance of angular momentum, through $\boldsymbol{\sigma} = \boldsymbol{\sigma}^T$, and
 277 balance of mass, through $\partial\rho/\partial t + \rho(\nabla \cdot \mathbf{v}_{\text{sb}}) = 0$. One can also consider adding
 278 the balance of energy. The constitutive relations for describing the soft-body
 279 material usually rely on both elastic and hyperelastic models, or ad-hoc con-
 280 stitutive models. These ad-hoc constitutive relations can originate from e.g.,
 281 phenomenological experiments of a specimen and provide an accurate simula-
 282 tion of the soft body deformation [4]. Note that hyperelastic models sometimes
 283 have many parameters that are difficult to identify in practice. Moreover, other
 284 phenomena such as viscosity, plasticity or anisotropy need also to be consid-
 285 ered into the constitutive equations. Anisotropy has, for example, a direct
 286 influence on the kinematics of the soft robot [5]. Finally, these deformation

287 models are very sensitive to the boundary conditions, thus to the modeling of
288 the actuators but also to external interactions.

289 All the three actuation strategies, tendons, fluidic actuators, and smart
290 materials, can be adopted in conjunction with continuum solid mechanics.
291 Their coupling with the soft body is obtained through the term \mathcal{C}_{int} . This can
292 be constituted by Lagrange multipliers $\mathcal{C}_{\text{int}} = \mathbf{\Lambda}^T \mathcal{I}_e + \mathbf{\Theta}^T \mathcal{I}_i$ arising from a set
293 of constraints imposed by the actuators on the soft body. They can also be
294 imposed as a set of boundary conditions for equation (1).

295 Solution strategies rely on numerical methods, e.g., finite and spectral ele-
296 ment methods, whereby the partial differential equations are solved at a set
297 of prescribed nodes (or mesh). This is typically extremely expensive compu-
298 tationally, with a corresponding number of degrees of freedom in the order of
299 $\mathcal{O}(N^3)$, where N is the number of nodes of the underlying mesh.

300 Successful implementations in the realm of soft robotics applications exist.
301 The software *SOFA* implements the finite element method to simulate con-
302 tinuum solid mechanics [6], and offers solutions, such as model reduction [7],
303 to find a compromise between accuracy and computation time. *ChainQueen*
304 implements a differentiable Lagrangian-Eulerian physical simulator based on
305 the moving least square material point method for solid mechanics, along
306 with actuation and contact with external objects [8]. *Evosoro* uses a solid
307 mechanics engine, *Voxelyze* [9], that allows the simulation of soft multi-
308 material robots [10]. These three options are open-source and currently under
309 active development. Some additional commercial software to tackle the internal
310 interaction modeling challenge exist, including *ABAQUS* [11], *ANSYS* [12],
311 *COMSOL* [13], and *Altair* [14], among others. These provide platforms for
312 solving full complexity solid mechanics problems, but they are not tailored to
313 soft robotics.

314 This modeling approach, along with the computational strategies for solv-
315 ing it, allows the description of all topologies commonly required in soft
316 robotics, e.g., rods, lattice of beams, shells, volumes. These topologies can be
317 generated by means of Computer-Aided Design (CAD), and standard meshing
318 practices. This however, may lead to an inexact geometrical representation of
319 the soft body, that in turn can yield an inaccurate solution for the soft-body
320 motion. This drawback could be addressed by using accurate mesh genera-
321 tion practices (e.g., high-order mesh generation [15, 16]) and by increasing the
322 number of mesh nodes, or with isogeometric analysis [17].

323 *2.2.2 Shell and rod models*

324 A significant number of soft robots are characterized by an elongated structure
325 with two dimensions much smaller compared to the third one. In this case, it
326 is possible to significantly reduce the number of degrees of freedom required to
327 describe the robot by adopting 1D rod models. Sometimes, only one dimension
328 is negligible, and 2D shell models may be adopted. These fall under the realm
329 of continuum mechanics although not in 3D.

330 A continuum modelling approach used in soft robotics is the Cosserat mod-
331 eling approach, particularly useful to describe rods and shells. Here, we focus
332 on this specific model, while acknowledging that there exist several others in
333 practice, both for rods and shells. In the Cosserat model, the material point
334 is replaced by a set of infinitesimal micro-solids stacked along the dominant
335 dimension [18] that ensures high accuracy in simulating the geometric nonlin-
336 earities arising from the finite deformation of the robot [19]. The mathematical
337 formalism underlying a Cosserat model relies on the Lie group of rigid body
338 transformation $SE(3)$, due to the assumptions made on the microstructures.
339 Following [20], if we consider rods, a Cosserat rod is modeled by a contin-
340 uous set of rigid cross sections stacked along a material line parameterized

341 by a curvilinear coordinate $\mathbf{x} = X \in [0, 1]$ to which a cross-sectional frame
 342 $\mathcal{F}(X) = (O, t_1, t_2, t_3)(X)$ is attached, where $O(X)$ is on the midline, $t_1(X)$ is
 343 a unit normal vector perpendicular to the cross-section, and $t_2(X)$ and $t_3(X)$
 344 are the unit vectors spanning the cross-sectional plane (see Fig. 3(b)).

345 The balance of momentum underlying this model can be recast within
 346 equation (1), where:

347 \mathcal{D} becomes $\partial/\partial t$, the partial derivative with respect to time t ,

348 \mathbf{q}_{sb} becomes $[v, \omega]^T$, the velocity twist field of the soft-body composed of
 349 the linear and angular velocity, respectively,

350 \mathcal{N} becomes $[\mathcal{N}_{\text{sb},v}, \mathcal{N}_{\text{sb},\omega}]$, with

351 $\mathcal{N}_{\text{sb},v} = 1/(\rho A)(\partial n/\partial x + \bar{n})$, and

352 $\mathcal{N}_{\text{sb},\omega} = (I^{-1}/\rho)(-\omega \times (\rho I \omega) + \partial c/\partial X + \partial r/\partial X \times n + \bar{c})$.

353 In the above equations, ρ is the density of the medium, I is the moment of
 354 inertia, A is the area of the cross section, r is the position vector of $O(X)$, while
 355 n and c are the linear and angular cross-sectional stresses along the beam.

356 Tendon actuators can be easily modeled in this framework as active internal
 357 wrenches \mathcal{C}_{int} that act directly on the cross-sectional stress. Similar equations
 358 can be derived for Cosserat shells [21]. This modeling framework is not suit-
 359 able for inflated chambers and some kind of smart material actuations, that
 360 inherently require a 3D description of the soft body.

361 Solution strategies for Cosserat-like models require the use of numerical
 362 methods, as they belong to the realm of continuum mechanics. To this end,
 363 methods introduced in the previous section are all suitable, i.e., finite and
 364 spectral element methods, and they are usually formulated in generalized coor-
 365 dinates. More recently, Cosserat models have been formulated in their strong
 366 form (as opposed to weak form, that is the basis for finite and spectral element

367 methods) on tree-like structures, thanks to the use of reduced coordinates. An
368 approach that has been traditionally applied in robotics.

369 In addition to the many research papers based on the Cosserat approach,
370 few software and toolboxes have been proposed recently. *Elastica* [22] is a
371 free and open-source software, which provides a discrete differential geometry
372 approximation of the Cosserat rod model. *SoRoSim* [23] is a MATLAB toolbox
373 that implements a strain-parametrization of tendon-driven soft robotic arms.
374 A piecewise-constant strain approximation has also been included as a plug-in
375 in *SOFA* [24].

376 Although Cosserat-like rod and shell models guarantee a good accuracy
377 for soft robots with one or two main dimensions (e.g., slender bodies) under-
378 going finite deformation, they are not suitable for full 3D soft robot body
379 deformations.

380 *2.2.3 Finite-dimensional parametrization models*

381 The previous models derive from continuum solid mechanics, therefore they
382 lead to sets of partial differential equations, as described in sections 2.2.1 and
383 2.2.2, that are computationally expensive to solve. It is also possible to describe
384 the behaviour of the soft body via finite dimensional models. These rely on a
385 description of the soft body that leverages a suitably parametrized central axis
386 or “backbone curve”, that assumes a prescribed expression. This description
387 leads to sets of ordinary differential equations in contrast to partial differential
388 equations produced by the previous two modeling strategies.

389 The parametrization of the backbone curve can be defined as follows. Each
390 frame $\mathcal{F}(X)$ described in the previous section can be viewed as an element of
391 the group of special Euclidean transformations (i.e., rigid-body displacements).
392 The origin of this frame traces out the backbone curve as the curvilinear coord-
393 inate X varies. The tangent to this curve is the normal to the cross-sectional

394 plane, $t_1(X)$ (see Fig. 3(c)). For each fixed value of time, the combined rigid-
 395 body instantaneous translational and rotational rate of change with respect
 396 to arclength is defined by matrix $\Theta(X) = [\mathcal{F}(X)]^{-1}(\partial\mathcal{F}(X)/\partial X)$ where
 397 $\mathcal{F}(X)$ is the roto-translational matrix describing the orientation and transla-
 398 tion of the frame (relative to the world frame at the base of the robot), with
 399 components $\mathbf{R}(X)$ and $\mathbf{p}(X)$, respectively [25–27]. In the case when the back-
 400 bone curve is inextensible (not stretchable), then there is coupling between
 401 the rotation matrix and the position vector. For instance, if the tangent to
 402 the soft robot arm at its base is $\mathbf{e}_1 = [1, 0, 0]^T$, then the tangent at X will
 403 be $\mathbf{R}(X)\mathbf{e}_1$ and integrating the tangent along the curve generates the posi-
 404 tion as $\mathbf{p}(X) = \int_0^X \mathbf{R}(s)\mathbf{e}_1 ds$. In general, it is always possible to use $\Theta(X)$,
 405 that is a coordinate-free parametrization. However, when there is coupling
 406 between the rotation matrix and the position vector, one can use an alter-
 407 native parametrization of the backbone curve by expanding rates of rotation
 408 parameters such as Euler angles. In the planar case, they reduce to the same
 409 parametrization.

410 The matrix $\Theta(X)$ has embedded in it information about instantaneous
 411 rotational and translational changes as a function of arclength, which can be
 412 extracted to form a vector $\mathbf{q}_{\text{sb}} = [v \ \omega]^T$ alluded to in the previous section.
 413 The vector $\mathbf{q}_{\text{sb}} = [v \ \omega]^T$ can then be expanded using a modal approach,
 414 that describes the spatio-temporal behavior of v and ω . This modal expan-
 415 sion is commonly defined as $\mathbf{q}_{\text{sb}}(X, t) = \sum_{i=1}^n \Phi_i(X)a_i(t)$, where $\Phi_i(X)$ are
 416 modes describing the spatial behaviour of the system, and $a_i(t)$ are coefficients
 417 describing its evolution in time. The v -part of this vector describes how the
 418 backbone curve stretches and how adjacent planar sections shear relative to
 419 each other. The ω -part of this vector describes bending and twisting, and is
 420 related to the classical concepts of curvature and torsion of space curves. The

421 modal expansion includes as a special case piecewise-constant curvature mod-
 422 els by choosing some functions $\Phi_i(X)$ to be piecewise constant for some values
 423 of X and equal to zero for others, as described in [26].

424 The parametrization and modal expansion introduced lead to a set of ordi-
 425 nary differential equations, that can be written using the formalism introduced
 426 in equation (1), where

427 \mathcal{D} becomes d/dt , the total derivative with respect to time t ,

428 $\widehat{\mathbf{q}}_{\text{sb}}$ becomes $[v \ \omega]^T$, and

429 \mathcal{N} becomes $-1/\mathbf{M}[\mathbf{D}(\mathbf{s}_{\text{sb}}, \mathbf{q}_{\text{sb}}) + \mathbf{K}(\mathbf{s}_{\text{sb}})]$, where \mathbf{s}_{sb} is the displacement of the
 430 soft body.

431 The nonlinear term just introduced is derived from the robot dynamic model,
 432 where \mathbf{M} is the inertial matrix, \mathbf{D} is a dissipative term that includes internal
 433 friction and other dissipative forces (such as Coriolis forces), and \mathbf{K} is an elastic
 434 term that encapsulate the stiffness of the system.

435 The coupling with actuation is achieved via an appropriate choice of the
 436 modal expansion, and it is commonly represented via $\mathcal{C}_{\text{int}} = \boldsymbol{\alpha}$, where $\boldsymbol{\alpha}$ is
 437 the vector of actuation forces. For example, when motors specify the angles
 438 between rigid links of a traditional robot, the modes would be Dirac delta
 439 functions in ω to describe revolute joints or in v to describe prismatic joints,
 440 and the weights would be the joint angles. In this sense, the modal approach
 441 can be used not only for soft/continuum robots but also for ones composed of
 442 rigid links, as well as hybrids.

443 The solution of the models in section 2.2.2 requires the use of numerical
 444 methods, e.g., finite and spectral element approximations. In contrast, solution
 445 methods for ordinary differential equations arising in this section are based on
 446 iterative schemes that update the weights $a_i(t)$ in time. These involve inverse
 447 Jacobian iterations as described in the articles listed earlier in this section.

448 The computational benefit of this approach is that instead of solving partial
449 differential equations, it averages properties over each section and reduces the
450 problem to a finite number of ordinary differential equations. This approach
451 has been applied to hyper-redundant manipulators of all kinds (i.e., those
452 consisting of a large number of rigid links, continuum filament, soft) over the
453 past several decades. Successful implementation in the realm of soft robotics
454 applications exist [28, 29].

455 *2.2.4 Data-driven and machine learning models*

456 An alternative approach to the models above is the use of machine learn-
457 ing techniques. In robotics, learning has been widely used for building the
458 kinematic and dynamic relations between a robot actuators and its position
459 in space. Neural networks have been used to this aim, mainly for control
460 purposes, implementing so-called neuro-controllers. In the same way, in soft
461 robots, neural networks can be used to learn the soft body dynamics and solve
462 the transformations from the actuator space to the space of the soft body
463 deformation and position. Following the formalism in equation (1), one tries
464 to learn the nonlinear and the coupling term for internal interactions, \mathcal{N} and
465 \mathcal{C}_{int} . This results in learning the right-hand side of equation (1) in one go, with
466 e.g., a neural network (NN): $\mathcal{D}\mathbf{q}_{\text{sb}} = \text{NN}[\mathbf{q}_{\text{sb}}(k) \rightarrow \mathbf{q}_{\text{sb}}(k + 1)]$, where k are
467 different time instances.

468 In [30], an analysis is given of how learning-based blocks can replace some
469 of the steps of the longer transformation chain involved in soft robot con-
470 trol. Diverse network topologies and learning paradigms can be used for this
471 purpose. In [31], a quantitative survey is presented, showing how supervised
472 learning is more widely used than unsupervised or reinforcement learning,
473 with references to the different techniques used. The survey presented in

474 [32] describes the learning techniques used for obtaining the mapping from
 475 actuation space to task space in continuum robots.

476 An interesting comparison between a model-based and a learning-based
 477 approach to the control of a same soft robot arm is presented in [33]. While the
 478 model-based method is more accurate in controlling the end-effector position,
 479 as resulting in simulation, its error tends to increase together with the model
 480 inaccuracies, e.g. fabrication inaccuracies. The learning-based controller error
 481 tends to be insensitive to such modeling inaccuracies, especially if training is
 482 accomplished on the physical robot arm.

483 Looking ahead, we envisage a promising direction of progress in the inte-
 484 gration of modeling techniques with machine learning, where models can feed
 485 neural networks and learning can replace specific sub-system mappings.

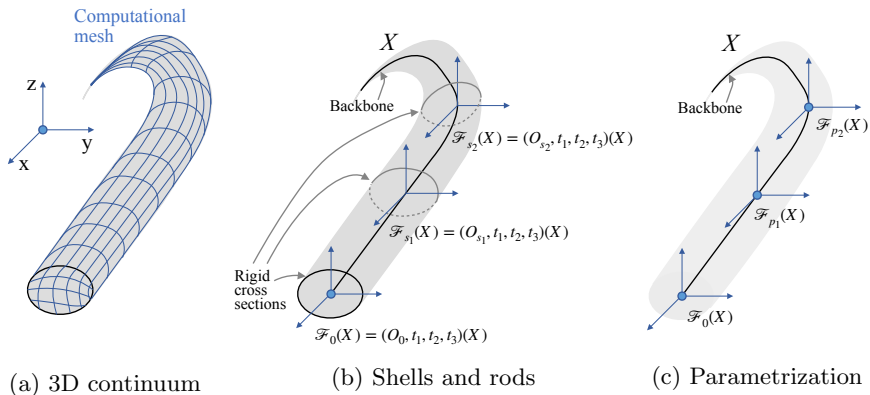


Fig. 3: A conceptual illustration of the models for internal interactions described in section 2, applied to the octopus arm of Fig. 2. (a) A representation of the mesh description in 3D continuum mechanics models. (b) Cosserat’s approach for rods. (c) Finite-dimensional parametrization models.

3 External interactions

3.1 Challenges

To benefit from embodied intelligence, we require medium–robot interaction modeling that can grasp the emergence of sensory–motor behaviour from the interplay with the surrounding environment. Modeling these external interactions, and coupling them with the internal interactions discussed in the previous section, closes the gap required to modeling the physics of embodied intelligence.

The task when modeling external interactions is to capture the complex, time-varying forces between the actuated soft-robot structures and the surrounding medium. The dynamics of fluids and deformable solids are generally nonlinear and unsteady, and interactions between the soft robot and the medium may create complex feedback loops and hysteresis effects. The key challenges to modeling external interactions are:

1. the multiphysics nature of the problem, that requires substantial interdisciplinary efforts, and
2. the partially known interfacial physics and unmodeled dynamics (e.g., nonlinear friction and turbulent drag).

In the following, we focus on medium-robot interaction, that we denote with the coupling term \mathcal{C}_{ext} introduced in equation (1). Here, the surrounding medium is either a fluid or a solid. The robot (i.e. the soft body) is assumed to be described by the models presented in section 2, along with its actuation. In general, any of the soft-body models in section 2 can be used in conjunction with the models introduced next, unless otherwise specified.

510 **3.2 Fluid models**

511 When fluid forces acting on a robot have a tangible impact on movement, as
512 with the octopus in Fig. 2, modeling fluid–robot interaction becomes essential.
513 Here the task is to capture the complex, time-varying, bidirectional forces
514 between the actuated soft robot structures and the surrounding fluid flow. To
515 this end, the field of fluid–structure interaction [34] is a key cross-discipline
516 that should be taken into account.

517 We describe three main modeling strategies, that can be adopted in the
518 context of fluid–robot interaction. These include continuum fluid mechanics
519 models, simplified lumped parameter models, and the relatively new field of
520 machine learning for flow modeling. We remark that we keep the description
521 at a general level, and we avoid entering into details that may hinder grasping
522 the essence of these modeling strategies.

523 *3.2.1 Continuum fluid mechanics models*

In analogy to continuum solid mechanics, the equations governing flow physics in a continuum setting can be considered as the most general model of a fluid interacting with the soft body described in section 2 (see Fig. 4(a)). The equations describing continuum fluid mechanics are the Navier-Stokes equations, constituted, in the most general case, by conservation of mass, momentum and energy. From a soft robot perspective, the action of the fluid modeled by the Navier-Stokes equations emerges in the form of equality constraints at the interface between the soft body and the fluid, denoted by $\Gamma_{\text{sb,f}}$.

In particular, we can write these interface constraints as follows:

$$\mathcal{I}_{e,f} = \begin{cases} \mathbf{q}_{sb} = \mathbf{q}_f & \text{on } \Gamma_{sb,f} & (2a) \\ \boldsymbol{\sigma}_{sb} \cdot \mathbf{n} = \boldsymbol{\sigma}_f \cdot \mathbf{n} & \text{on } \Gamma_{sb,f} & (2b) \\ \mathbf{x}_{sb} = \mathbf{x}_f & \text{on } \Gamma_{sb,f}. & (2c) \end{cases}$$

524 In equation (2), $\mathbf{q}_{sb} = \mathbf{v}_{sb}$ corresponds to the velocity of the soft body, and
 525 $\mathbf{q}_f = \mathbf{v}_f$ is the velocity of the fluid at the interface $\Gamma_{sb,f}$, \mathbf{n} is the normal at any
 526 soft body location, $\boldsymbol{\sigma}_f$ is the fluid Cauchy stress tensor composed of the sum of
 527 the deviatoric stress tensor $\boldsymbol{\tau}^{(f)}$ (that accounts for the viscosity) and a pressure
 528 term $-p\mathbf{I}$, and \mathbf{x}_{sb} and \mathbf{x}_f are the positions of the soft body and fluid inter-
 529 faces, respectively. The solution for the solid velocity is achieved through the
 530 modeling strategies introduced in section 2. The solution for the fluid velocity
 531 is instead obtained by solving the Navier-Stokes equations. For the purpose of
 532 this article, we report the momentum equation, that can be written as follows
 533 $\partial(\rho_f \mathbf{q}_f)/\partial t + \nabla \cdot (\rho_f \mathbf{q}_f \otimes \mathbf{q}_f) = \nabla \cdot \boldsymbol{\sigma}_f + \boldsymbol{\beta}_f$, where ρ_f is the fluid density, and $\boldsymbol{\beta}_f$
 534 is a forcing term acting on the fluid (e.g., gravity). Depending on the nature
 535 of the problem, we can have several approximations, including incompressible
 536 Navier-Stokes equations, where the density is a constant, compressible Navier-
 537 Stokes equations, where the density is not constant and the flow might develop
 538 shock waves, thin-layer Navier-Stokes equations, that describes flow in thin
 539 layers, and potential flow equations that describe irrotational flows, to cite a
 540 few.

541 The compatibility conditions in equation (2) can enter into the equations
 542 describing the soft body (1) as Lagrange multipliers $\mathcal{C}_{ext} = \boldsymbol{\Lambda}^T \mathcal{I}_{e,f}$, or being
 543 imposed as external equality constraints $\mathcal{I}_{e,f}$ or as boundary conditions. Given
 544 the nature of the coupling, the majority of the soft body models presented in

545 section 2 may be used, with the due approximations required for coupling. For
546 instance, in the case of continuum solid mechanics (section 2.2.1), the com-
547 patibility conditions are applied to the interface nodes between the soft body
548 mesh and the fluid mesh (or a proxy representing the interface, if the soft
549 body / fluid nodes are not matching). In this case, there exist two mainstream
550 approaches for coupling: partitioned and monolithic. The former uses a struc-
551 tural and a fluid solver iteratively until convergence, while the latter solves a
552 fully coupled system of equations in one go [35]. When using continuum fluid
553 mechanics in conjunction with simplified methods, such as finite-dimensional
554 parametrization models (section 2.2.3), one instead needs to lump the effect
555 of the fluid solution into a set of degrees of freedom compatible with the finite
556 expansions used to describe the deformation of the body.

557 In terms of solution strategies, there exist well-established approaches in
558 the realm of fluid–structure interaction methods. The two main approaches
559 are conforming and non-conforming methods [35]. The former enforces
560 equations (2b) and (2c), while the latter enforces equation (2a). Conforming
561 methods can be used in conjunction with partitioned methods, where a popular
562 algorithm is the arbitrary Lagrangian Eulerian approach [36]. Non-conforming
563 methods are typically used in conjunction with monolithic methods, where a
564 popular algorithm is the immersed boundary method [37–39].

565 While the successful implementation of continuum fluid mechanics and its
566 interaction with soft bodies have been largely explored in biology [40, 41], in
567 soft robotics it is still nascent. One of the key challenges is the computational
568 costs of the simulations and an accurate coupling with the soft body dynamics
569 and actuation system. To solve the equations arising in this modeling strategy,
570 there exist both commercial and open-source multiphysics packages. These
571 include ANSYS [12] and COMSOL [13], Altair [14], Flow3D [42], Adina [43],

572 and OpenFOAM [44], to cite a few. However, these are not readily tuned for
 573 soft robotics applications. For example, implementing actuation strategies in
 574 a nonlinear elastic material interacting with a fluid described by the Navier-
 575 Stokes equations remain challenging.

576 Continuum fluid mechanics can fully capture the effect that a fluid has on
 577 a soft robot. However, their inherent computational costs make these models
 578 prohibitive to use for practical design and control purposes, and they have
 579 found limited use in soft robotics, as of today. As computational resources
 580 become more available and underlying algorithms more efficient, the scope of
 581 these models will expand and they may be eventually used for design and
 582 control purposes. Yet, today they can already be adopted for high-fidelity sim-
 583 ulations that can grasp the complex behaviour of biological systems interacting
 584 with a fluid, and extract the key physical principles underlying their embodied
 585 intelligence. These principles can in turn improve simplified and less expensive
 586 models used for design and control.

587 *3.2.2 Lumped parameter models*

588 In some circumstances, it is acceptable and convenient to simplify the descrip-
 589 tion of the fluid interacting with the soft body. In these cases, one no longer
 590 solves the equations governing continuum fluid mechanics, but aggregates
 591 the overall effect of the fluid into a set of lumped contributions. The main
 592 lumped contributions consist of added mass, drag/lift forces, and buoyancy
 593 (see Fig. 4(b)). These can be included as forces into the coupling term \mathcal{C}_{ext} as
 594 follows: $\mathcal{C}_{\text{ext}} = \mathbf{f}_{\text{added mass}} + \mathbf{f}_{\text{drag}} + \mathbf{f}_{\text{lift}} + \mathbf{f}_{\text{buoyancy}}$, where the subscript of each
 595 term is self-explanatory. The added mass, $\mathbf{f}_{\text{added mass}}$, is the virtual mass or
 596 inertia added to the soft robot due its need to move the fluid surrounding it. For
 597 instance, if the soft body was a simple sphere immersed in an incompressible
 598 fluid, the added mass would be equal to $\mathbf{f}_{\text{added mass}} = \rho_f V_{\text{sb}} [\mathbf{D}\mathbf{q}_f/\mathbf{D}t - \mathbf{d}\mathbf{q}_{\text{sb}}/\mathbf{d}t]$,

599 where $D\mathbf{q}_f/Dt$ is the material derivative of the fluid velocity, $d\mathbf{q}_{sb}/dt$ is the
600 total derivative of the spherical soft body velocity, ρ_f is the fluid density and
601 V_{sb} is the volume of the spherical soft robot. Drag and lift forces are typically
602 proportional to the velocity of the fluid flowing around the soft body, and they
603 can be calculated as $\mathbf{f}_{drag} = (1/2)\rho_f \mathbf{q}_f A_{sb} C_{drag}$, and $\mathbf{f}_{lift} = (1/2)\rho_f \mathbf{q}_f A_{sb} C_{lift}$,
604 where A_{sb} is the area of the soft body exposed to the fluid, and C_{drag} and
605 C_{lift} are the drag and lift coefficients that, for simplified geometries, are com-
606 monly tabulated. Finally, the buoyancy term is typically accounted for as a
607 net vertical force composed by buoyancy plus gravity.

608 The term \mathcal{C}_{ext} just defined enters into the right-hand side of the soft-body
609 equation (1) as a forcing term, and can be used in conjunction with any of the
610 models presented in section 2. Obviously, the lumped contributions need to
611 correctly interface with the degrees of freedom of the soft body. In the case of
612 continuum solid mechanics models, (i.e., the ones introduced in sections 2.2.1
613 and 2.2.2), the lumped forces need to be distributed onto the nodes under-
614 lying the discretization of the soft body. Similarly, for finite-dimensional
615 parametrization models (i.e., the ones introduced in section 2.2.3), \mathcal{C}_{ext} needs
616 to be applied to the degrees of freedom of the functional parametrization
617 adopted.

618 The coupling term \mathcal{C}_{ext} , and its constitutive components, (i.e., added mass,
619 lift, drag and buoyancy) depend on the shape of the soft body, and therefore
620 they can change over time as effect of actuations or interactions with the envi-
621 ronment. Employing such changes to increase efficiency, to direct behaviours,
622 or to improve performances is key to establish quantitative advantages of soft
623 robotics.

624 In practice, the forces expressed in \mathcal{C}_{ext} are often coupled with continuum
625 solid models of soft robots (i.e., the ones described in section 2.2.1 and 2.2.2),

626 such that a complete coupling between continuum fluid mechanics models and
627 continuum solid mechanical models is generally not performed due to its com-
628 putational costs. Successful implementation of these strategies in soft robotics
629 has been performed, for example in [45].

630 Eventually, even if external forces are included without modelling the con-
631 tinuum of the fluid, the dependence of such forces on shape-varying coefficients
632 allows reaching a trade-off between accuracy and relevance of simulation, with
633 the computational power available for modelling. Depending on the goal of
634 the simulation, this is similar to fluid–structure interaction in the aerospace
635 industry: while complete coupled simulations are used for design, flight simu-
636 lators employ a similar coupling to match fidelity of simulation with real-time
637 computation.

638 *3.2.3 Data-driven and machine learning models*

639 Recent data-driven and machine learning methods have become widely used
640 for modeling complex fluids [46–48]. Several recent approaches have leveraged
641 machine learning to direct speed up high-fidelity simulation of the Navier-
642 Stokes equations, especially the ones involving turbulence [49–52]. Indeed, for
643 complex flows, it is often impractical to resolve all scales of the flow, and
644 instead researchers employ turbulence models, such as the Reynolds aver-
645 aged Navier-Stokes (RANS) equations or large eddy simulation (LES). These
646 approximate the smaller scales, and allow for less computationally expensive
647 simulations of the Navier-Stokes equations. Machine learning is rapidly advanc-
648 ing these computational fields [46], providing enhanced data-driven turbulence
649 closures [53–57]. For even further reduction in computation, it is often possible
650 to develop reduced-order models (ROMs) that are tailored to a specific flow
651 and provide an optimal balance between accuracy and efficiency. Reduced-
652 order models are typically at least partially data-driven, as they are based on

653 modal decompositions [58], and they have close connections to machine learn-
654 ing. Several recent approaches have provided more accurate and generalizable
655 ROMs, for example based on sparse regression [59–63] and the use of deep
656 neural networks to learn effective coordinate systems [64]. Other promising
657 recent techniques for physics computation based on machine learning include
658 physics-informed neural networks [65] and deep operator networks [66].

659 In addition to using machine learning techniques to develop surrogate
660 models for the complex fluid environment, there is also a need to model dis-
661 crepancies that arise in complex multiphysics applications. The equations of
662 a simple fluid are relatively well understood, but interfacial dynamics, non-
663 Newtonian fluids, and multiphase flows all pose significant modeling challenges
664 even to represent the fundamental physical effects in a full-fidelity model, let
665 alone in a reduced-order model. There are considerable efforts to use machine
666 learning approaches to model these discrepancies between observed data and
667 idealized physical models.

668 **3.3 Solid models**

669 A model of solid–robot interaction should accurately capture how normal
670 forces, tangential forces or friction, and adhesion/cohesion forces affect and
671 can therefore be leveraged by the soft body. To this end, contact mechan-
672 ics [67] and tribology [68] represent the key broad cross-disciplines for modeling
673 solid–robot interaction.

674 In the following, we outline the main modeling strategies that can be
675 adopted in the context of solid–robot interaction. These include the use of
676 continuum solid mechanics to model a deformable solid, simplified lumped
677 parameter models, and more recent machine learning strategies. A key for these
678 models to be accurate is related to the frictional interaction, and consequent
679 constraints at the interface between the solid and the soft robot.

3.3.1 Continuum three-dimensional solid mechanics models

The models underlying continuum solid mechanics have been introduced in section 2.2.1, albeit for the soft robot. These models can be used also to describe a surrounding deformable solid medium (see Fig. 4(c)). Its interaction with the soft robot is described by the coupling term \mathcal{C}_{ext} introduced in equation (1). This is typically the result of a series of constraints that need to be satisfied at the interface between the soft robot and the solid medium. Such constraints are similar to the one introduced in section 3.2.1, except that they need to account for complementarities, that is, when the system transition from no contact to contact, or from static friction (i.e., no tangential relative movement between two elastic surfaces) to dynamic friction (i.e., relative tangential movement).

For instance, the normal contact between two elastic surfaces can be modeled using the Signorini's framework, that uses a distance function S_n to measure the distance between two surfaces along the normal direction. Signorini's formulation can be written as $S_n(\mathbf{q}) \perp \boldsymbol{\sigma}_n$, where $\boldsymbol{\sigma}_n$ is the stress along the normal direction \mathbf{n} at the contact interface, and the symbol \perp denotes complementarity: if $S_n(\mathbf{q}) > 0$ then $\boldsymbol{\sigma}_n = 0$ (no contact); if $S_n(\mathbf{q}) = 0$ then $\boldsymbol{\sigma}_n > 0$ (contact). Tangential or frictional contact can instead be modeled using the Coulomb's law framework, where the complementarity is given by the relation $\boldsymbol{\sigma}_t = \mu_s \boldsymbol{\sigma}_n$. Here, complementarity arises from static vs. dynamic friction. For $\boldsymbol{\sigma}_t \leq \boldsymbol{\sigma}_{\text{max}}$ there is static friction (no relative sliding of the two surfaces), while for $\boldsymbol{\sigma}_t > \boldsymbol{\sigma}_{\text{max}}$ there is dynamic friction (relative sliding of the two surfaces), where $\boldsymbol{\sigma}_{\text{max}}$ is the maximum value of stress that allow static friction.

These interface conditions need to be encapsulated into the continuum solid mechanics models describing the soft robot and the elastic solid medium interacting with the robot, in a similar manner as described in section 3.2.1,

707 for the constraints in equation (2). They can for instance be embedded into
708 the equations through the term $\mathcal{C}_{\text{ext}} = \Lambda \mathcal{I}_{e,s}$, using Lagrange multipliers for
709 the constraints. However, in contrast to section 3.2.1, one needs to account for
710 the complementarities in the contact and friction laws. These complementarities
711 create jumps in velocities. When the coupled system transitions from one
712 regime to another (e.g., from no contact to contact, or from static to dynamic
713 friction), the inertial terms underlying the system of equations is not defined.

714 In order to solve this contact problem, it is necessary to rely on numerical
715 methods that account for these complementarities, and the singularities they
716 produce. To this end, a strategy is first to calculate $S_n(\mathbf{q})$ using a measurement
717 of proximity distance, interpenetration distance, interpenetration volumes, or a
718 precise measurement of the moment and the contact configuration between two
719 simulation steps. Following this detection, a set of constraints are defined, often
720 on contact points (but one can extend to volumes or to non-planar surfaces).
721 Finally, the solution can be obtained with different numerical strategies such as
722 Lagrange multipliers, penalty methods and augmented Lagrangian methods, in
723 conjunction with optimization solvers dedicated to complementarity problems.
724 The time-integration of the resulting equations is achieved via event-driven
725 methods that account for the singularity in the underlying equations – see e.g.,
726 [69], [70].

727 An example of successful implementation of this strategy can be found
728 in [71]. Here, the contact problem is formulated to solve an inverse model for
729 the control of a soft robot, which leads to writing a quadratic problem with
730 complementarity constraints (also referred to as QPCC).

731 Most of the major multiphysics computational software previously cited,
732 including ABAQUS [11], ANSYS [12] and COMSOL [13], can be used to solve
733 contact between two elastic solids, yet they are not necessarily tailored to

734 soft robotics applications. In the article [72], a literature review of physical
735 engines for simulation in robotic applications is listed, most of these engines
736 support contact modeling. On the other hand, not all engines are adapted
737 to deformable robots, in particular to simulate volume deformations. We can
738 note the SOFA software [73], originally dedicated to medical simulation, offers
739 plug-ins dedicated to soft robotics and proposes implementations of FEM and
740 Cosserat rods that are compatible with contact modeling.

741 Similar considerations as for continuum fluid mechanics can be made. In
742 particular, these models are computationally expensive, and they may lead
743 to impractical solutions for soft robotics applications today, especially in the
744 context of real-time control.

745 *3.3.2 Lumped parameter models*

746 Similarly to what we have introduced for fluid models, we can consider a
747 simplified approach, where we can aggregate the effect of contact between
748 two surfaces into lumped contributions. For instance, when the external solid
749 can be considered rigid, one can introduce some simplifications to the model
750 outlined in section 3.3.1. In particular, the state \mathbf{q}_s of a rigid body can be rep-
751 resented by the position of its center of mass, its orientation, and its linear and
752 angular velocity (see Fig. 4(d)). Once these are known, it is possible to formu-
753 late the rigid-robot interaction problem. This implies identifying the point of
754 contact between the soft body and the rigid solid, and applying an equivalent
755 frictional force \mathbf{f} and torque $\boldsymbol{\tau}$, induced by the interaction between the soft
756 and the rigid body. The interaction surface between the rigid solid and the
757 soft robot is typically modeled as a planar surface. This leads to models that
758 contain only the three degrees of freedom associated to frictional forces at the
759 planar surface, \mathbf{f} .

760 In practice, a soft robot interacting with a rigid body leads to non-planar
 761 contact surfaces, with multiple points of contact. This introduces three addi-
 762 tional degrees of freedom, and provide a six-dimensional model for the normal
 763 and frictional wrenches, as both force \mathbf{f} and torque $\boldsymbol{\tau}$ are three-dimensional.
 764 Following the formalism adopted in [74], one can define the normal force
 765 and torque as $\mathbf{f}_n = -\int_S p \cdot \mathbf{n} dS$, and $\boldsymbol{\tau}_n = -\int_S p \cdot [(\mathbf{r} \times \mathbf{n})] dS$, respec-
 766 tively, and the frictional force and torque as $\mathbf{f}_t = -\mu \int_S p \cdot \mathbf{v}_r dS$, and
 767 $\boldsymbol{\tau}_t = -\mu \int_S p \cdot [\mathbf{r} \times \mathbf{v}_r] dS$, respectively, where S is the contact surface, \mathbf{v}_r is the
 768 relative velocity between the rigid solid and the soft robot, \mathbf{n} is the normal to
 769 the contact surface, \mathbf{r} is the torque arm, p is the contact pressure distribution,
 770 and μ is the friction coefficient.

771 The coupling is achieved by encapsulating these forces and torques into the
 772 coupling term \mathcal{C}_{ext} . This acts as a forcing term on the right-hand side of the
 773 soft body equation, that is $\mathcal{C}_{\text{ext}} = \mathbf{f}_n + \boldsymbol{\tau}_n + \mathbf{f}_t + \boldsymbol{\tau}_t$.

774 The computational costs associated with these models are relatively small
 775 compared to the interaction between two deformable solids.

776 Applications of this modeling strategies in soft robotics exists, both in
 777 terms of analytical approaches [75, 76] and computational models [6, 77], that
 778 focused on simulating contact behaviours of soft robot grasping and manipu-
 779 lation as well as crawling [78, 79]. Inverse model of soft robot in situation of
 780 frictionless contact [71] and adhesive contact situations has been investigated
 781 for control of manipulation and locomotion [80].

782 These models can be broadly applied for describing several tasks involv-
 783 ing the interaction of the soft robot with e.g., rigid solids, and similar
 784 considerations as in section 3.2.2 can be made.

785 *3.3.3 Data-driven and machine learning models*

786 Frictional and normal contact modeling is notoriously difficult, and a high
787 prediction accuracy is onerous to achieve, especially for soft-bodied robots that
788 interact with environments or objects with vastly different surface properties.

789 Recent efforts explore the augmentation of simulation representations with
790 neural networks to close sim-to-real gaps (see, e.g., [81–84]), reducing the
791 uncertainty that contact with unknown objects or environments introduces.

792 A naive approach is to learn the mapping of the previous to the next state
793 directly. This would mean that the nonlinear equations \mathcal{N} in equation (1),
794 and also the actuation and constraint force terms, are replaced with a neural
795 network.

796 However, this is all but practical for complex robots, and it is best to
797 acquire data for interactions, such as frictional contact, that lead to predic-
798 tion inaccuracies in our state-of-the-art models, and to only learn corrections.
799 More specifically, we could learn corrections for the frictional forces that act
800 on the soft-body, improving a first-order estimate that we get from a known
801 simulation representation. For augmentation tasks, it is desirable to work with
802 a differentiable simulation representation [85].

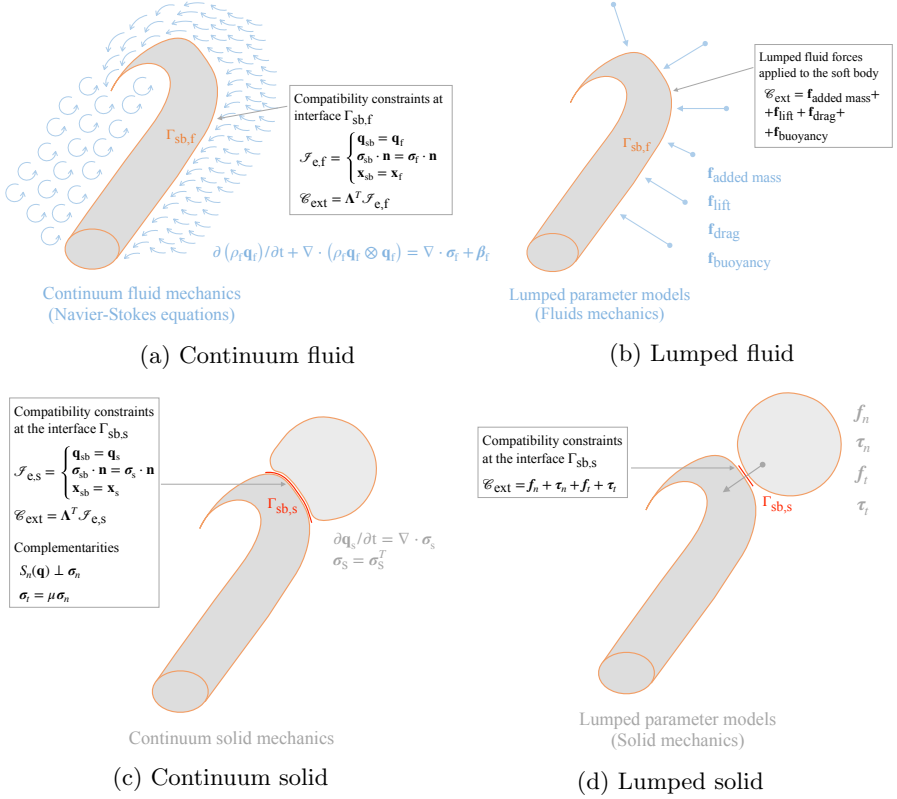


Fig. 4: A conceptual illustration of the models for external interactions described in section 3, applied to the octopus arm of Fig. 2. (a) Continuum fluid mechanics models. (b) Lumped fluid models. (c) Continuum solid mechanics models. (d) Lumped solid models.

803 4 From models to practice

804 As emerging from the previous sections, presenting the models involved in
 805 describing soft robots and embodied intelligence inside a unified framework
 806 is challenging, yet helpful. Therefore, it is not surprising that a structured
 807 modeling framework for the physics of interactions in soft robotics remains
 808 elusive.

809 The models presented range from high-dimensional (sections 2.2.1, 2.2.2
810 for internal interactions, and sections 3.3.1, 3.2.1 for external interactions)
811 to low-dimensional (section 2.2.3 for internal interactions, and sections 3.3.2,
812 3.2.2 for external interactions). The former have found relatively little use in
813 soft robotics, due to their computational costs, hence limited applicability for
814 control and design purposes. The latter have been instead used with different
815 degrees of success due to their simplifications, that may be unable to capture
816 the rich physics of internal and external interactions.

817 High-dimensional models can provide a framework for simulation of internal
818 and external interactions. These simulations, in turn, can be used to under-
819 stand the principles behind an observed and/or desired behaviour and may
820 eventually be adopted for automatic design [78, 79, 86] in the future, if com-
821 putational power and algorithms will allow for a sufficiently fast model-driven
822 workflow. Yet, having these models permits constructing improved approxi-
823 mated and low-dimensional representations of soft robots, that capture their
824 overall behaviour at a cheaper computational cost, feasible for design and con-
825 trol purposes today. Indeed, the high-dimensional models can capture the key
826 components underpinning embodied intelligence physical principles, thereby
827 allowing for a more accurate low-dimensional description of how soft robots can
828 achieve the embodied intelligence of biological systems. As an example, Fig. 2
829 depicts a low-dimensional model for octopus' underwater locomotion [87]. A
830 low-dimensional description is typically constituted by a representation of the
831 behaviour of the system in a reduced space, composed by much fewer degrees of
832 freedom than the original high-dimensional counterpart [7, 88]. Therefore, one
833 must identify a suitable low-dimensional representation that retains a sufficient
834 accuracy to describe the whole system.

835 The discovery of low-dimensional representation (often referred to as fun-
836 damental or parsimonious models) is currently done empirically by observing
837 the system. Whether a high-dimensional model is available, the synthesis to
838 the lower-level counterpart (if any) can be obtained more systematically. Accu-
839 rately informed fundamental models can capture the overall behaviour of the
840 soft robot and expose a few key aggregate physical parameters to describe
841 a specific task (e.g., locomotion, arm movements, etc.). These fundamental
842 models provide a generic base upon which specific morphology/control could
843 be developed, following the template/anchor approach proposed in [89]. The
844 analysis of the fundamental models might increase the comprehension of the
845 system and expose quantitative advantages of compliant robots over rigid ones.

846 This concept was successfully employed in underwater legged robots, where
847 shape-dependent forces, elastic leg elements, and pushing-based actuation
848 interweave to shape the basin of attraction of the hopping limit cycle. Shape
849 morphing proved how deformable bodies can be exploited to overcome actu-
850 ation limits [90]. Another remarkable example is presented in [91], where the
851 elastic components of a soft robotic squid have been exploited to increase
852 swimming efficiency. A second-order forced oscillation model was developed to
853 catch the relationship between internal and external forces, mediated by actu-
854 ation frequency, in an approximate and simplified way. In both cases, they are
855 not a low-level counterpart of the models presented in section 2 and 3, but
856 they are fundamental models which capture the specific behavior of interest,
857 and can provide insights into the design of actual soft robots.

858 Finally, please note that, for all the three main scopes of internal interac-
859 tions and external interactions with fluid and solid media, we discussed how
860 machine learning techniques can be used to solve the same modeling problems.

861 5 Conclusions

862 We walked through the quest for modelling soft robots with a focus on how
863 to describe the physics involved in their embodied intelligence. We argue that
864 modelling the deformations of a soft robot body under internal actuation forces
865 and external interaction forces can capture the practical essence of embodied
866 intelligence. We described the mathematical models used for describing such
867 internal and external interactions in a soft robot body, including related soft-
868 ware tools, and we discussed how to use them in practice. For the first time, we
869 show a unified view of the multiphysics of interactions arising from embodied
870 intelligence, and we link them to the design of soft robots.

871 Tables 1, and 2 summarize this analysis and provides a practical guidance
872 to the modelling methods that can be beneficially used in soft robotics (not
873 including machine learning techniques), enabling soft robots to fully lever-
874 age on embodied intelligence, acquire unprecedented abilities and respond to
875 unmet needs, ultimately contributing to further soft robotics progress.

876 We argue that, in contrast to the current trial (physically build the robot)
877 and error (robot testing) approach, soft-robot design can transition to a
878 model-informed workflow. Indeed, prototype-driven design (also referred to as
879 trial-and-error) was likely the fastest and most efficient way to proceed, espe-
880 cially in the soft robotics exploratory phase. Today, we are at a stage where
881 computational modelling within a model-driven umbrella can enable (i) scaling
882 up soft-robot design in response to application needs, (ii) holistic model-based
883 control embedding external interactions, and (iii) high-fidelity simulations,
884 opening the path towards soft-robot digital twins.

885 This transition is within grasp, in an interdisciplinary dialogue of roboti-
886 cists with communities like computational physics, applied mathematics,
887 scientific computing and machine learning. This unified approach will allow soft

888 robotics to thrive in the next few decades and establish itself as a model-driven
 889 scientific discipline that can tangibly impact human activities.

Table 1: Summary of models for soft body mechanics and internal interactions, with reference to equation (1). As discussed in Section 2.2.4, machine learning techniques can be also proposed to solve the same modeling problems.

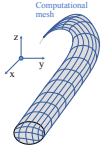
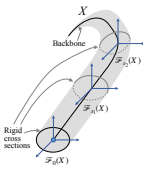
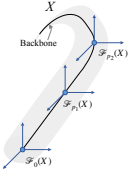
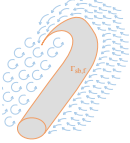
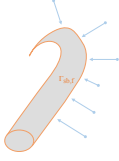
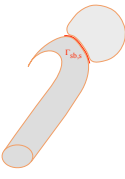
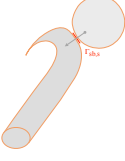
Model	\mathcal{D}	\mathbf{q}_{sb}	\mathcal{N}_{sb}	C_{int}	Software tools
Continuum 3D solid mechanics  section 2.2.1	$\partial/\partial t$	\mathbf{v}_{sb}	$\nabla \cdot \boldsymbol{\sigma}_{sb}$	Actuation imposed as equality and inequality constraints: $\mathcal{I}_e, \mathcal{I}_i$, through $\boldsymbol{\Lambda}^T \mathcal{I}_e + \boldsymbol{\Theta}^T \mathcal{I}_i$ (e.g., Lagrange multipliers) [used with 1D, 2D, 3D actuations]	<i>SOFA</i> [6] <i>ChainQueen</i> [8] <i>Evosoro</i> [10] <i>Voxelize</i> [9] <i>ABAQUS</i> [11] <i>ANSYS</i> [12] <i>COMSOL</i> [13] <i>Altair</i> [14]
Rods and shells, e.g., Cosserat  section 2.2.2	$\partial/\partial t$	$[v, \omega]^T$	$[\mathcal{N}_{sb,v}, \mathcal{N}_{sb,\omega}]^T$ $\mathcal{N}_{sb,v} = 1/(\rho A)(\partial n/\partial x + \bar{n})$ $\mathcal{N}_{sb,\omega} = I^{-1}/\rho[-\omega \times (\rho I \omega) + \partial c/\partial X + \partial r/\partial X \times n + \bar{c}]$	Actuation imposed as active internal wrenches $\boldsymbol{\alpha}, \boldsymbol{\tau}$ [used with 1D, 2D actuation]	<i>SOFA</i> [6] <i>Elastica</i> [22] <i>SoRoSim</i> [23]
Finite-dimensional parametrization  section 2.2.3	d/dt	$[v \ \omega]^T$	$-1/\mathbf{M} [\mathbf{D}(\mathbf{s}_{sb}, \mathbf{q}_{sb}) + \mathbf{K}(\mathbf{s}_{sb})]$ \mathbf{s}_{sb} is the displacement of the soft body	Actuator forces grouped in a vector $\boldsymbol{\alpha}$ that acts as a forcing term on the right-hand side [used with 1D actuation]	Bespoke tools written in various languages

Table 2: Summary of models for external interactions, with reference to equation (1). As discussed in sections 3.2.3 and 3.3.3, machine learning techniques can be also proposed to solve the same modeling problems.

Fluid models	\mathcal{C}_{ext}	Software tools
Continuum fluid mechanics  section 3.2.1	Compatibility constraints at interface $\Gamma_{\text{sb},f}$: $\mathcal{I}_{e,f} = \begin{cases} \mathbf{q}_{\text{sb}} = \mathbf{q}_f \\ \boldsymbol{\sigma}_{\text{sb}} \cdot \mathbf{n} = \boldsymbol{\sigma}_f \cdot \mathbf{n} \\ \mathbf{x}_{\text{sb}} = \mathbf{x}_f \end{cases}$ $\mathcal{C}_{\text{ext}} = \Lambda^T \mathcal{I}_{e,f}$ (e.g., Lagrange multipliers) Segregated, monolithic approaches	ANSYS [12] COMSOL [13] Altair [14] Flow3D [42] Adina [43] OpenFOAM [44]
Lumped parameters  section 3.2.2	Fluid forces applied on the right-hand side of equation (1) as aggregated contributions $\mathbf{f}_{\text{added mass}} + \mathbf{f}_{\text{drag}} + \mathbf{f}_{\text{lift}} + \mathbf{f}_{\text{buoyancy}}$	Bespoke tools written in various languages
Solid models	\mathcal{C}_{ext}	Software tools
Continuum solid mechanics  section 3.3.1	Compatibility constraints at interface $\Gamma_{\text{sb},s}$: $\mathcal{I}_{e,s} = \begin{cases} \mathbf{q}_{\text{sb}} = \mathbf{q}_s \\ \boldsymbol{\sigma}_{\text{sb}} \cdot \mathbf{n} = \boldsymbol{\sigma}_s \cdot \mathbf{n} \\ \mathbf{x}_{\text{sb}} = \mathbf{x}_s \end{cases}$ $\mathcal{C}_{\text{ext}} = \Lambda^T \mathcal{I}_{e,s}$ (e.g., Lagrange multipliers) Complementarities $S_n(\mathbf{q}) \perp \boldsymbol{\sigma}_n$ $\boldsymbol{\sigma}_t = \mu \boldsymbol{\sigma}_n$	SOFA [6] ABAQUS [11] ANSYS [12] COMSOL [13]
Lumped parameters  section 3.3.2	Normal and tangential forces and torques applied on the right-hand side of equation (1) as aggregated contributions $\mathbf{f}_n, +\boldsymbol{\tau}_n + \mathbf{f}_t + \boldsymbol{\tau}_t$	SOFA [6] and other bespoke tools written in various languages

890 **Acknowledgments** Gianmarco Mengaldo acknowledges NUS support
891 through his start-up grant (R-265-000-A36-133). Gregory Chirikjian acknowl-
892 edges MOE Tier I grant (R-265-000-655-114) and the NRF Medium Sized
893 Centre CARTIN allocation (R-261-521-002-592). Cecilia Laschi acknowledges
894 NUS support through her start-up grant (R-265-000-A31-133 and R-265-
895 000-A31-731) and the support of the National Research Foundation (NRF),
896 Singapore, under its Medium Sized Centre CARTIN - Centre for Advanced
897 Robotics Technology Innovation (R-261-521-001-592).

898 **References**

- 899 [1] Kim, S., Laschi, C., Trimmer, B.: Soft robotics: a bioinspired evolution in
900 robotics. *Trends in biotechnology* **31**(5), 287–294 (2013)
- 901 [2] Pfeifer, R., Lungarella, M., Iida, F.: Self-organization, embodiment, and
902 biologically inspired robotics. *science* **318**(5853), 1088–1093 (2007)
- 903 [3] Blickhan, R., Seyfarth, A., Geyer, H., Grimmer, S., Wagner, H., Günther,
904 M.: Intelligence by mechanics. *Philosophical Transactions of the Royal
905 Society A: Mathematical, Physical and Engineering Sciences* **365**(1850),
906 199–220 (2007)
- 907 [4] Xavier, M.S., Fleming, A.J., Yong, Y.K.: Finite element modeling of soft
908 fluidic actuators: Overview and recent developments. *Advanced Intelligent
909 Systems* **3**(2), 2000187 (2021)
- 910 [5] Vanneste, F., Goury, O., Duriez, C.: Enabling the control of a new degree
911 of freedom by using anisotropic material on a 6-dof parallel soft robot. In:
912 *Robosoft 2021* (2021)

- 913 [6] Duriez, C., Bieze, T.: Soft robot modeling, simulation and control in real-
914 time. In: *Soft Robotics: Trends, Applications and Challenges*, pp. 103–109
915 (2017)
- 916 [7] Goury, O., Duriez, C.: Fast, generic, and reliable control and simulation of
917 soft robots using model order reduction. *IEEE Transactions on Robotics*
918 **34**(6), 1565–1576 (2018)
- 919 [8] Hu, Y., Liu, J., Spielberg, A., Tenenbaum, J.B., Freeman, W.T., Wu,
920 J., Rus, D., Matusik, W.: Chainqueen: A real-time differentiable physical
921 simulator for soft robotics. In: *2019 International Conference on Robotics*
922 *and Automation (ICRA)*, pp. 6265–6271 (2019)
- 923 [9] Hiller, J., Lipson, H.: Dynamic simulation of soft multimaterial 3d-printed
924 objects. *Soft robotics* **1**(1), 88–101 (2014)
- 925 [10] Cheney, N., MacCurdy, R., Clune, J., Lipson, H.: Unshackling evolution:
926 evolving soft robots with multiple materials and a powerful generative
927 encoding. *ACM SIGEVolution* **7**(1), 11–23 (2014)
- 928 [11] ABAQUS software. [https://www.3ds.com/products-services/simulia/
929 products/abaqus/](https://www.3ds.com/products-services/simulia/products/abaqus/). Accessed: 2021-10-27
- 930 [12] ANSYS software. <https://www.ansys.com>. Accessed: 2021-10-27
- 931 [13] COMSOL software. <https://www.comsol.com>. Accessed: 2021-10-27
- 932 [14] Altair software. <https://www.altair.com>. Accessed: 2021-10-27
- 933 [15] Turner, M., Peiró, J., Moxey, D.: Curvilinear mesh generation using a
934 variational framework. *Computer-Aided Design* **103**, 73–91 (2018)

- 935 [16] Mengaldo, G., Moxey, D., Turner, M., Moura, R.C., Jassim, A., Taylor,
936 M., Peiro, J., Sherwin, S.J.: Industry-relevant implicit large-eddy simu-
937 lation of a high-performance road car via spectral/hp element methods.
938 arXiv preprint arXiv:2009.10178 (2020)
- 939 [17] Cottrell, J.A., Hughes, T.J.R., Bazilevs, Y.: Isogeometric Analysis:
940 Toward Integration of CAD and FEA
- 941 [18] Eringen, A.C.: Microcontinuum Field Theories: I. Foundations and Solids,
942 (2012)
- 943 [19] Antman, S.: Nonlinear Problems of Elasticity. Applied Mathematical
944 Sciences. Springer, ??? (2006)
- 945 [20] Boyer, F., Lebastard, V., Candelier, F., Renda, F.: Dynamics of contin-
946 uum and soft robots: A strain parameterization based approach. IEEE
947 Transactions on Robotics **37**(3), 847–863 (2020)
- 948 [21] Boyer, F., Renda, F.: Poincaré’s equations for cosserat media: Application
949 to shells. Journal of Nonlinear Science **27**(1), 1–44 (2017)
- 950 [22] Gazzola, M., Dudte, L., McCormick, A., Mahadevan, L.: Forward and
951 inverse problems in the mechanics of soft filaments. Royal Society open
952 science **5**(6), 171628 (2018). <https://doi.org/10.1098/rsos.171628>
- 953 [23] Mathew, A.T., Hmida, I.B., Armanini, C., Boyer, F., Renda, F.: Sorosim:
954 a matlab toolbox for soft robotics based on the geometric variable-strain
955 approach. arXiv preprint arXiv:2107.05494 (2021)
- 956 [24] Adagolodjo, Y., Renda, F., Duriez, C.: Coupling numerical deformable
957 models in global and reduced coordinates for the simulation of the direct

- 958 and the inverse kinematics of soft robots. *IEEE Robotics and Automa-*
959 *tion Letters* **6**(2), 3910–3917 (2021). [https://doi.org/10.1109/LRA.2021.](https://doi.org/10.1109/LRA.2021.3061977)
960 [3061977](https://doi.org/10.1109/LRA.2021.3061977)
- 961 [25] Fu, Q., Gatt, S.W., Mitchel, T.W., Kim, J.S., Chirikjian, G.S., Li, C.:
962 Lateral oscillation and body compliance help snakes and snake robots sta-
963 bly traverse large, smooth obstacles. *Integrative and comparative biology*
964 **60**(1), 171–179 (2020)
- 965 [26] Chirikjian, G.S., Burdick, J.W.: A modal approach to hyper-redundant
966 manipulator kinematics. *IEEE Transactions on Robotics and Automation*
967 **10**(3), 343–354 (1994)
- 968 [27] Kim, B., Ha, J., Park, F.C., Dupont, P.E.: Optimizing curvature sensor
969 placement for fast, accurate shape sensing of continuum robots. In: 2014
970 IEEE International Conference on Robotics and Automation (ICRA), pp.
971 5374–5379 (2014). IEEE
- 972 [28] Suzumori, K., Iikura, S., Tanaka, H.: Development of flexible microac-
973 tuator and its applications to robotic mechanisms. In: Proceedings.
974 1991 IEEE International Conference on Robotics and Automation, pp.
975 1622–1623 (1991). IEEE Computer Society
- 976 [29] Webster III, R.J., Jones, B.A.: Design and kinematic modeling of con-
977 stant curvature continuum robots: A review. *The International Journal*
978 *of Robotics Research* **29**(13), 1661–1683 (2010)
- 979 [30] George Thuruthel, T., Ansari, Y., Falotico, E., Laschi, C.: Control strate-
980 gies for soft robotic manipulators: A survey. *Soft robotics* **5**(2), 149–163
981 (2018)

- 982 [31] Kim, D., Kim, S.-H., Kim, T., Kang, B.B., Lee, M., Park, W., Ku, S.,
983 Kim, D., Kwon, J., Lee, H., *et al.*: Review of machine learning methods
984 in soft robotics. *Plos one* **16**(2), 0246102 (2021)
- 985 [32] Wang, X., Li, Y., Kwok, K.-W.: A survey for machine learning-based
986 control of continuum robots. *Frontiers in Robotics and AI*, 280 (2021)
- 987 [33] Giorelli, M., Renda, F., Calisti, M., Arienti, A., Ferri, G., Laschi, C.:
988 Neural network and jacobian method for solving the inverse statics of a
989 cable-driven soft arm with nonconstant curvature. *IEEE Transactions on*
990 *Robotics* **31**(4), 823–834 (2015)
- 991 [34] Dowell, E.H., Hall, K.C.: Modeling of fluid-structure interaction. *Annual*
992 *review of fluid mechanics* **33**(1), 445–490 (2001)
- 993 [35] Hou, G., Wang, J., Layton, A.: Numerical methods for fluid-structure
994 interaction—a review. *Communications in Computational Physics* **12**(2),
995 337–377 (2012)
- 996 [36] Souli, M., Benson, D.J.: *Arbitrary Lagrangian Eulerian and Fluid-*
997 *structure Interaction: Numerical Simulation*. John Wiley & Sons, ???
998 (2013)
- 999 [37] Mittal, R., Iaccarino, G.: Immersed boundary methods. *Annu. Rev. Fluid*
1000 *Mech.* **37**, 239–261 (2005)
- 1001 [38] Taira, K., Colonius, T.: The immersed boundary method: a projection
1002 approach. *Journal of Computational Physics* **225**(2), 2118–2137 (2007)
- 1003 [39] Goza, A., Colonius, T.: A strongly-coupled immersed-boundary formula-
1004 tion for thin elastic structures. *Journal of Computational Physics* **336**,

1005 401–411 (2017)

1006 [40] Dickinson, M.H., Farley, C.T., Full, R.J., Koehl, M., Kram, R., Lehman,
1007 S.: How animals move: an integrative view. *science* **288**(5463), 100–106
1008 (2000)

1009 [41] Lauder, G.V.: Fish locomotion: recent advances and new directions.
1010 *Annual review of marine science* **7**, 521–545 (2015)

1011 [42] FLOW3D software. <https://www.flow3d.com>. Accessed: 2021-10-27

1012 [43] Adina software. <http://www.adina.com>. Accessed: 2021-10-27

1013 [44] Weller, H.G., Tabor, G., Jasak, H., Fureby, C.: A tensorial approach
1014 to computational continuum mechanics using object-oriented techniques.
1015 *Computers in physics* **12**(6), 620–631 (1998)

1016 [45] Renda, F., Giorgio-Serchi, F., Boyer, F., Laschi, C., Dias, J., Seneviratne,
1017 L.: A unified multi-soft-body dynamic model for underwater soft robots.
1018 *The International Journal of Robotics Research* **37**(6), 648–666 (2018).
1019 <https://doi.org/10.1177/0278364918769992>

1020 [46] Duraisamy, K., Iaccarino, G., Xiao, H.: Turbulence modeling in the age
1021 of data. *Annual Reviews of Fluid Mechanics* **51**, 357–377 (2019)

1022 [47] Brunton, S.L., Noack, B.R., Koumoutsakos, P.: Machine learning for fluid
1023 mechanics. *Annual Review of Fluid Mechanics* **52**, 477–508 (2020)

1024 [48] Vinuesa, R., Brunton, S.L.: The potential of machine learning to enhance
1025 computational fluid dynamics. *arXiv preprint arXiv:2110.02085* (2021)

- 1026 [49] Bar-Sinai, Y., Hoyer, S., Hickey, J., Brenner, M.P.: Learning data-
1027 driven discretizations for partial differential equations. Proceedings of the
1028 National Academy of Sciences **116**(31), 15344–15349 (2019)
- 1029 [50] Kochkov, D., Smith, J.A., Alieva, A., Wang, Q., Brenner, M.P., Hoyer,
1030 S.: Machine learning accelerated computational fluid dynamics. arXiv
1031 preprint arXiv:2102.01010 (2021)
- 1032 [51] Wang, R., Walters, R., Yu, R.: Incorporating symmetry into deep dynam-
1033 ics models for improved generalization. arXiv preprint arXiv:2002.03061
1034 (2020)
- 1035 [52] Li, Z., Kovachki, N., Azizzadenesheli, K., Liu, B., Bhattacharya, K., Stu-
1036 art, A., Anandkumar, A.: Fourier neural operator for parametric partial
1037 differential equations. arXiv preprint arXiv:2010.08895 (2020)
- 1038 [53] Ling, J., Kurzawski, A., Templeton, J.: Reynolds averaged turbulence
1039 modelling using deep neural networks with embedded invariance. Journal
1040 of Fluid Mechanics **807**, 155–166 (2016)
- 1041 [54] Maulik, R., San, O., Rasheed, A., Vedula, P.: Subgrid modelling for two-
1042 dimensional turbulence using neural networks. Journal of Fluid Mechanics
1043 **858**, 122–144 (2019)
- 1044 [55] Novati, G., de Laroussilhe, H.L., Koumoutsakos, P.: Automating turbu-
1045 lence modelling by multi-agent reinforcement learning. Nature Machine
1046 Intelligence **3**(1), 87–96 (2021)
- 1047 [56] Beetham, S., Capecelatro, J.: Formulating turbulence closures using
1048 sparse regression with embedded form invariance. Physical Review Fluids
1049 **5**(8), 084611 (2020)

- 1050 [57] Beetham, S., Fox, R.O., Capecehatro, J.: Sparse identification of multi-
1051 phase turbulence closures for coupled fluid–particle flows. *Journal of Fluid*
1052 *Mechanics* **914** (2021)
- 1053 [58] Taira, K., Brunton, S.L., Dawson, S., Rowley, C.W., Colonius, T., McK-
1054 eon, B.J., Schmidt, O.T., Gordeyev, S., Theofilis, V., Ukeiley, L.S.: Modal
1055 analysis of fluid flows: An overview. *AIAA Journal* **55**(12), 4013–4041
1056 (2017)
- 1057 [59] Brunton, S.L., Proctor, J.L., Kutz, J.N.: Discovering governing equations
1058 from data by sparse identification of nonlinear dynamical systems.
1059 *Proceedings of the National Academy of Sciences* **113**(15), 3932–3937
1060 (2016)
- 1061 [60] Loiseau, J.-C., Brunton, S.L.: Constrained sparse Galerkin regression.
1062 *Journal of Fluid Mechanics* **838**, 42–67 (2018)
- 1063 [61] Loiseau, J.-C., Noack, B.R., Brunton, S.L.: Sparse reduced-order mod-
1064 eling: sensor-based dynamics to full-state estimation. *Journal of Fluid*
1065 *Mechanics* **844**, 459–490 (2018)
- 1066 [62] Deng, N., Noack, B.R., Morzynski, M., Pastur, L.R.: Low-order model for
1067 successive bifurcations of the fluidic pinball. *Journal of fluid mechanics*
1068 **884**(A37) (2020)
- 1069 [63] Deng, N., Noack, B.R., Morzyński, M., Pastur, L.R.: Galerkin force model
1070 for transient and post-transient dynamics of the fluidic pinball. *Journal*
1071 *of Fluid Mechanics* **918** (2021)
- 1072 [64] Lee, K., Carlberg, K.T.: Model reduction of dynamical systems on
1073 nonlinear manifolds using deep convolutional autoencoders. *Journal of*

- 1074 Computational Physics **404**, 108973 (2020)
- 1075 [65] Raissi, M., Perdikaris, P., Karniadakis, G.E.: Physics-informed neural
1076 networks: A deep learning framework for solving forward and inverse
1077 problems involving nonlinear partial differential equations. Journal of
1078 Computational Physics **378**, 686–707 (2019)
- 1079 [66] Lu, L., Jin, P., Pang, G., Zhang, Z., Karniadakis, G.E.: Learning nonlinear
1080 operators via deeponet based on the universal approximation theorem of
1081 operators. Nature Machine Intelligence **3**(3), 218–229 (2021)
- 1082 [67] Johnson, K.L., Johnson, K.L.: Contact Mechanics. Cambridge university
1083 press, ??? (1987)
- 1084 [68] Vakis, A.I., Yastrebov, V.A., Scheibert, J., Nicola, L., Dini, D., Minfray,
1085 C., Almqvist, A., Paggi, M., Lee, S., Limbert, G., *et al.*: Modeling and
1086 simulation in tribology across scales: An overview. Tribology International
1087 **125**, 169–199 (2018)
- 1088 [69] Studer, C., Glocker, C.: Simulation of non-smooth mechanical systems
1089 with many unilateral constraints. Proceedings ENOC-2005 Eindhoven
1090 (2005)
- 1091 [70] Acary, V.: Projected event-capturing time-stepping schemes for nons-
1092 mooth mechanical systems with unilateral contact and coulomb’s friction.
1093 Computer Methods in Applied Mechanics and Engineering **256**, 224–250
1094 (2013)
- 1095 [71] Coevoet, E., Escande, A., Duriez, C.: Optimization-based inverse model
1096 of soft robots with contact handling. IEEE Robotics and Automation
1097 Letters **2**(3), 1413–1419 (2017)

- 1098 [72] Collins, J., Chand, S., Vanderkop, A., Howard, D.: A review of physics
1099 simulators for robotic applications. *IEEE Access* (2021)
- 1100 [73] sofa framework. <https://www.sofa-framework.org>. Accessed: 2021-11-22
- 1101 [74] Xu, J., Aykut, T., Ma, D., Steinbach, E.: 6dls: Modeling nonplanar
1102 frictional surface contacts for grasping using 6-d limit surfaces. *IEEE*
1103 *Transactions on Robotics* (2021)
- 1104 [75] Xydias, N., Kao, I.: Modeling of contact mechanics and friction limit
1105 surfaces for soft fingers in robotics, with experimental results. *The*
1106 *International Journal of Robotics Research* **18**(9), 941–950 (1999)
- 1107 [76] Majidi, C., Shepherd, R.F., Kramer, R.K., Whitesides, G.M., Wood, R.J.:
1108 Influence of surface traction on soft robot undulation. *The International*
1109 *Journal of Robotics Research* **32**(13), 1577–1584 (2013)
- 1110 [77] Deimel, R., Brock, O.: A novel type of compliant and underactu-
1111 ated robotic hand for dexterous grasping. *The International Journal of*
1112 *Robotics Research* **35**(1-3), 161–185 (2016)
- 1113 [78] Lipson, H., Pollack, J.B.: Automatic design and manufacture of robotic
1114 lifeforms. *Nature* **406**(6799), 974–978 (2000)
- 1115 [79] Hiller, J., Lipson, H.: Automatic design and manufacture of soft robots.
1116 *IEEE Transactions on Robotics* **28**(2), 457–466 (2011)
- 1117 [80] Coevoet, E., Escande, A., Duriez, C.: Soft robots locomotion and manipu-
1118 lation control using fem simulation and quadratic programming. In: 2019
1119 2nd IEEE International Conference on Soft Robotics (RoboSoft), pp.
1120 739–745 (2019)

- 1121 [81] Hwangbo, J., Lee, J., Dosovitskiy, A., Bellicoso, D., Tsounis, V., Koltun,
1122 V., Hutter, M.: Learning agile and dynamic motor skills for legged robots.
1123 *Science Robotics* **4**(26) (2019)
- 1124 [82] Golemo, F., Taiga, A.A., Courville, A., Oudeyer, P.-Y.: Sim-to-real trans-
1125 fer with neural-augmented robot simulation. In: *Conference on Robot*
1126 *Learning*, pp. 817–828 (2018). PMLR
- 1127 [83] Battaglia, P., Pascanu, R., Lai, M., Jimenez Rezende, D., et al.: Interac-
1128 tion networks for learning about objects, relations and physics. *Advances*
1129 *in neural information processing systems* **29** (2016)
- 1130 [84] Jiang, Y., Liu, K.: Data-augmented contact model for rigid body simula-
1131 tion (2018)
- 1132 [85] Bächer, M., Knoop, E., Schumacher, C.: Design and control of soft robots
1133 using differentiable simulation. *Current Robotics Reports* **2**(2), 211–221
1134 (2021). <https://doi.org/10.1007/s43154-021-00052-7>
- 1135 [86] Lipson, H.: Challenges and opportunities for design, simulation, and
1136 fabrication of soft robots. *Soft Robotics* **1**(1), 21–27 (2014)
- 1137 [87] Calisti, M., Laschi, C.: Morphological and control criteria for self-stable
1138 underwater hopping. *Bioinspiration & biomimetics* **13**(1), 016001 (2017)
- 1139 [88] Chenevier, J., González, D., Aguado, J.V., Chinesta, F., Cueto, E.:
1140 Reduced-order modeling of soft robots. *PloS one* **13**(2), 0192052 (2018)
- 1141 [89] Full, R.J., Koditschek, D.E.: Templates and anchors: neuromechanical
1142 hypotheses of legged locomotion on land. *Journal of experimental biology*
1143 **202**(23), 3325–3332 (1999)

- 1144 [90] Picardi, G., Chellapurath, M., Iacoponi, S., Stefanni, S., Laschi, C., Cal-
1145 isti, M.: Bioinspired underwater legged robot for seabed exploration with
1146 low environmental disturbance. *Science Robotics* **5**(42) (2020)
- 1147 [91] Bujard, T., Giorgio-Serchi, F., Weymouth, G.D.: A resonant squid-
1148 inspired robot unlocks biological propulsive efficiency. *Science Robotics*
1149 **6**(50), 2971 (2021). <https://doi.org/10.1126/scirobotics.abd2971>